International Journal of Thermophysics, Vol. 17, No. 6, 1996

Simultaneous Measurements of Normal Spectral Emissivity by Spectral Radiometry and Laser Polarimetry at High Temperatures in Millisecond-Resolution Pulse-Heating Experiments: Application to Molybdenum and Tungsten

A. Cezairliyan,[1,2] S. Krishnan,[3] and J. L. McClure[1]

Received February 14, 1996

Spectral radiometry and laser polarimetry are two independent techniques for the measurement of spectral emissivity of materials. In this paper, a high-speed system is described for the rapid measurement of normal spectral emissivity of a specimen based on the simultaneous utilization of the two techniques. One of the goals of this work was to ascertain the accuracy of the laser polarimetry technique in measurement of normal spectral emissivity at high temperatures. To accomplish this goal, the normal spectral emissivities, in the vicinity of 0.633 μm, of molybdenum and tungsten were measured by the two techniques over the temperature range 2000 to 2800 K. The results obtained by the two techniques are in agreement within 1%. The total uncertainty (two-standard deviation level) in measurement of emissivity by either spectral radiometry or laser polarimetry technique is estimated to be not more than $\pm 2\%$.

KEY WORDS: high-speed measurements; high temperatures; laser polarimetry; molybdenum; normal spectral emissivity; pulse heating; pyrometry; radiation thermometry; spectral radiometry; tungsten.

1. INTRODUCTION

Normal spectral emissivity is not only an important property in its own right, but plays an essential role in the determination of the true temperature

[1] Metallurgy Division, National Institute of Standards and Technology, Gaithersburg, Maryland 20899, U.S.A.
[2] To whom correspondence should be addressed.
[3] Containerless Research, Inc., Evanston, Illinois 60201, U.S.A.

0195-928X/96/1100-1455$09.50/0

of a material from measurements of its radiance temperature utilizing radiation thermometry.

The most direct and widely considered as the most accurate method of determining normal spectral emissivity utilizes measurements of radiance from the surface of the material of interest and that from a blackbody cavity at the same temperature. In practice, this conventional radiometry method is generally best realized by having the specimen incorporate a blackbody and comparing the radiance from the adjacent surface of the specimen to that from the blackbody. However, this method has some serious drawbacks; it cannot be applied to specimens which either are too small or are inaccessible for the inclusion of a blackbody cavity. This method is also not applicable to uncontained (typically levitated) liquid materials.

Therefore, there is a strong need for a high-temperature technique which can be used to measure normal spectral emissivity independent of blackbody requirements, thus resolving the problem of true temperature measurements by radiation thermometry. One such method which has recently emerged is laser polarimetry. This method has been applied to measurements of the normal spectral emissivity of levitated liquid metals under steady-state conditions [1, 2].

The objectives of the present study were (a) to extend the laser polarimetry method to measurements on rapidly heated specimens in millisecond-resolution experiments and (b) to validate the laser polarimetry technique by performing experiments where the normal spectral emissivities of specimens (molybdenum and tungsten) are measured simultaneously by two different methods, namely, conventional spectral radiometry and novel laser polarimetry.

In the following sections, descriptions of the two methods, the measurement system, the measurements, the results, estimates of uncertainties, a discussion, and conclusions are presented. For brevity, in the rest of the paper, "emissivity" is used to mean "normal spectral emissivity" unless otherwise noted.

2. DESCRIPTION OF THE TWO METHODS

2.1. Measurement of Emissivity by Spectral Radiometry

In this method, emissivity, ε_λ, is obtained from the measurements of radiance, $I_{s,\lambda}$, from the surface of a specimen at a given wavelength, λ, and radiance, $I_{b,\lambda}$, from a blackbody cavity fabricated in the specimen. Normal spectral emissivity is defined as

$$\varepsilon_\lambda = \frac{I_{s,\lambda}}{I_{b,\lambda}} \qquad (1)$$

According to Planck's law

$$I_\lambda = \frac{c_1}{\lambda^5 (e^{c_2/\lambda T} - 1)} \tag{2}$$

where c_1 is the first radiation constant, c_2 is the second radiation constant, and λ is wavelength. Writing the above expression for both $I_{s,\lambda}$ and $I_{b,\lambda}$ and simplifying the result, one obtains the following relation for emissivity:

$$\varepsilon_\lambda = \frac{e^{c_2/\lambda T_{b,\lambda}} - 1}{e^{c_2/\lambda T_{s,\lambda}} - 1} \tag{3}$$

where $T_{b,\lambda}$ and $T_{s,\lambda}$ are blackbody and surface radiance temperatures, respectively, in K. Equation (3) can be used to obtain emissivity from measured values of the blackbody and surface radiance temperatures corresponding to the effective wavelength of the measuring instrument such as a radiation thermometer (optical pyrometer).

2.2. Measurement of Emissivity by Laser Polarimetry

In this method, emissivity, ε_λ, is obtained from the determination of spectral reflectivity, R_λ. For opaque materials, Kirchhoff's law states,

$$\varepsilon_\lambda = 1 - R_\lambda \tag{4}$$

Spectral reflectivity is given by

$$R_\lambda = \frac{(n - n_0)^2 + k^2}{(n + n_0)^2 + k^2} \tag{5}$$

where n is the real part of the index of refraction, n_0 is the refractive index of the transparent ambient medium at the material surface, and k is the extinction coefficient

To obtain n and k, the optical constants of the material of interest, the target surface is illuminated at a nonnormal angle of incidence with laser radiation of known incident polarization. The polarimeter, which is described in Section 3.4, measures the four Stokes parameters, S_0, S_1, S_2, and S_3, of the reflected radiation simultaneously. The Stokes parameters provide the complete description of the state of polarization of the radiation. If the incident polarization state is set to $+45°$ (linear), and the

reflected Stokes parameters are measured, the ellipsometric parameters, ψ and Δ, can be expressed as [3]

$$\psi = \frac{1}{2}\tan^{-1}\left[\frac{\sqrt{S_3^2 + S_2^2}}{-S_1}\right] \tag{6}$$

$$\Delta = \tan^{-1}\left[\frac{-S_3}{S_2}\right] \tag{7}$$

The values of ψ, Δ, and the angle of incidence, θ, yield the refractive index, n, and the extinction coefficient, k, of the reflecting materials according to the following equation:

$$n - ik = n_0 \tan(\theta)\left[1 - \frac{4\rho \sin^2(\theta)}{(1+\rho)^2}\right]^{1/2} \tag{8}$$

where $\rho = \tan(\psi)\exp(i\Delta)$ and n_0 is the refractive index of the transparent ambient medium.

Conventional methods of determining the polarization state of radiation are generally too slow and utilize designs with moving parts and therefore are not suitable for applications that require high measurement speeds. Recently, new polarimeter designs with stationary optical elements and four detectors have been developed [4, 5]. One such design, the division-of-amplitude photopolarimeter (DOAP), was employed for measurements of the emissivity of materials reported in this paper.

A complete description of the operation of the DOAP and its optical characteristics is given in the literature [4]. The instrument divides the incoming beam (reflected from the specimen) into four separate beams whose fluxes are simultaneously detected by four detectors. The instrument transforms the four-component Stokes vector, S_0, S_1, S_2, and S_3, which describes the incoming polarization state of incident radiation into four intensities, I_0, I_1, I_2, and I_3, measured at its four detectors according to the equation

$$I = MS \tag{9}$$

where S is the vector of the Stokes parameters, I is the vector of the measured intensities, and M is the 4×4 instrument matrix. If the instrument matrix is known, the unknown Stokes vector is determined by the inverse relation:

$$S = M^{-1}I \tag{10}$$

The instrument matrix is determined through a calibration process in which the response to radiation of different known polarization states is measured. The matrix which best matches the measured intensities to the known calibration states is then calculated. The calibration procedure for the DOAP has been described in the literature [4].

3. MEASUREMENT SYSTEM

3.1. General

The measurement system described in this paper permits the measurement of emissivity of a specimen by two independent techniques during millisecond-resolution pulse heating experiments. The specimens were in the form of thin-wall tubes with a small hole fabricated in the wall at the middle of the specimen length to approximate blackbody conditions.

For emissivity measurements utilizing the radiometry method, dual pyrometers were used. The first pyrometer always viewed the blackbody hole in the specimen, while the second pyrometer viewed the surface of the

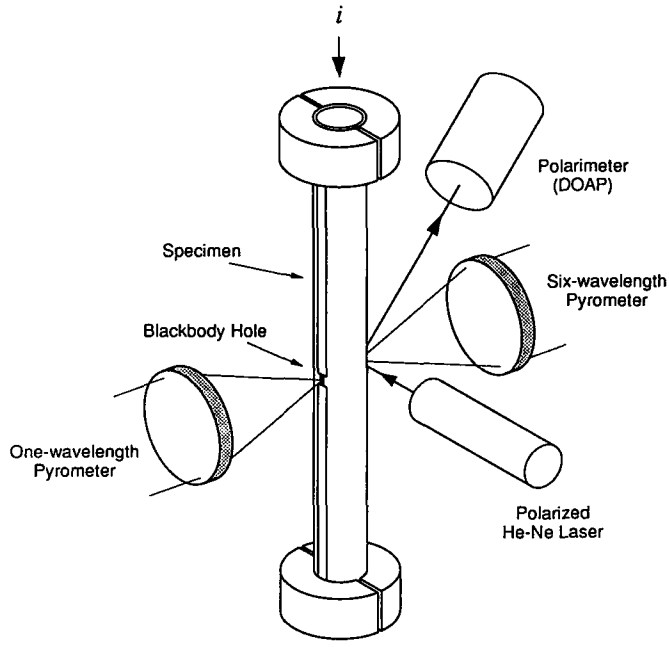

Fig. 1. Schematic diagram of the specimen and the configuration of the pyrometers and the polarimeter. Dimensions are not to scale.

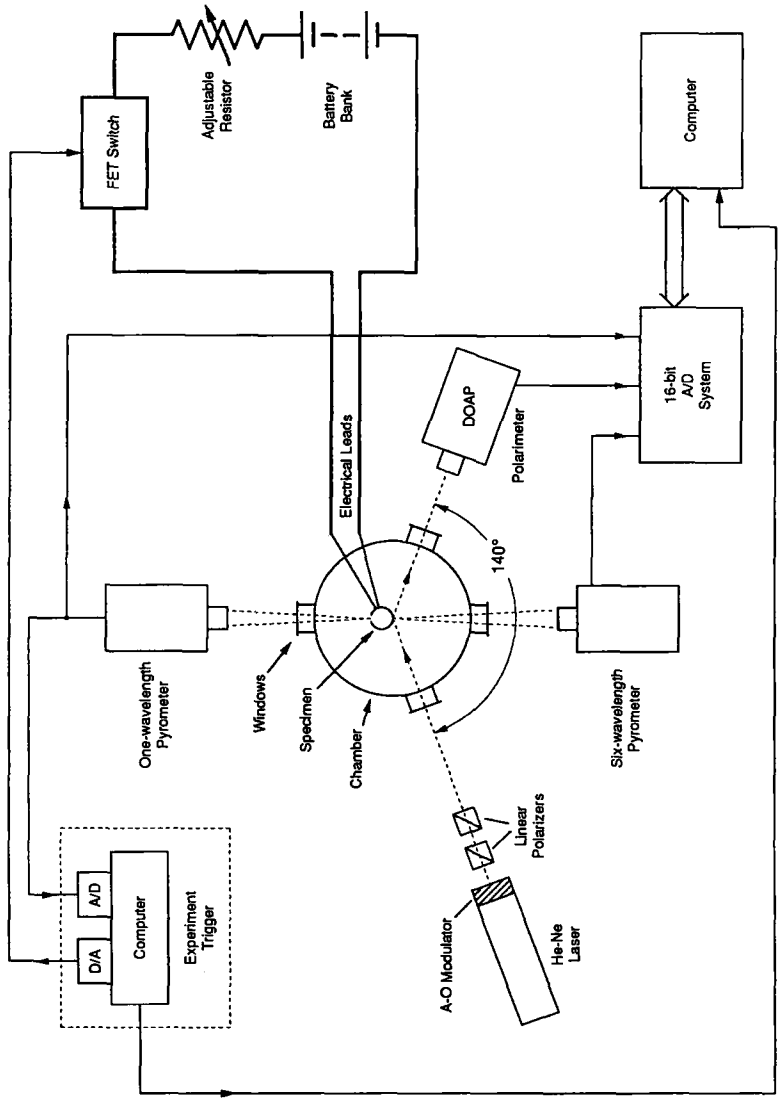

Fig. 2. Functional diagram of the overall experimental arrangement including the pulse-heating system and the radiometric and polarimetric instrumentation.

specimen at the same horizontal plane as that of the first pyrometer but on the side opposite the blackbody hole. For emissivity measurements utilizing the polarimetry method, a laser polarimeter was used. The laser target was close to the target of the second pyrometer. A schematic diagram of a specimen and the configuration of the pyrometers and the polarimeter is shown in Fig. 1.

The overall experimental arrangement (shown in Fig. 2) consists of the following: the pulse-heating system, the radiometry system, the polarimetry system, and the data acquisition system. They are described briefly in the following sections.

3.2. Pulse-Heating System

The pulse-heating system consisted of the specimen connected in series with a battery bank, an adjustable resistor (a water-cooled Inconel tube), and a fast-acting solid-state switch. The voltage (up to 48 V) of the battery bank and the length (hence, resistance) of the Inconel tube were adjusted to control the heating rate of the specimen. Details regarding the construction and operation of the basic pulse-heating system have been given in earlier publications [6, 7]. The solid-state (FET) switch [8] is a new addition to the system, replacing the original electromechanical switch. The timing of various events, such as closing/opening of the switch and triggering of electronic instruments, was controlled by means of a dedicated computer.

3.3. Radiometry System

The radiometry system consisted of two high-speed pyrometers. The first pyrometer, which viewed the blackbody hole in the specimen, operated at two wavelengths nominally at 0.65 and 1.5 μm [9]. However, in the present work, only the 0.65 μm channel was used. Therefore, for simplicity and to eliminate any possible confusion, this pyrometer is referred to as the one-wavelength pyrometer in the present paper. The target of this pyrometer was a circular area 0.2 mm in diameter. The second pyrometer, which viewed the surface of the specimen on the side opposite the blackbody hole, was a six-wavelength pyrometer [10]. This pyrometer was capable of measuring radiance temperature at six wavelengths in the nominal range 0.5 to 0.9 μm. However, for the present work, only two of the wavelengths, nominally 0.6 and 0.65 μm, were needed and thus used to bracket the wavelength (0.633 μm) of the polarimeter's He–Ne laser. The target of this pyrometer was a circular area 0.5 mm in diameter.

Both pyrometers were calibrated prior to the experiments. The 0.65 μm channels of both pyrometers were calibrated against a tungsten-filament

reference lamp, which, in turn, had been calibrated against the NIST Photoelectric Pyrometer by the Radiometric Physics Division at NIST. Subsequently, in the case of the six-wavelength pyrometer, temperature calibration of the 0.65-μm channel was transferred to the 0.6-μm channel by performing (steady-state) measurements on a graphite-tube blackbody furnace. All temperatures reported in this paper are based on the International Temperature Scale of 1990 (ITS-90) [11].

3.4. Polarimetry System

To enable performance of polarimetric measurements, the specimen chamber included two additional windows (12 mm in diameter, fine-annealed strain-free fused silica) whose included angle was 140° (see Fig. 2). Two optical rails supported the incident polarization optics and the analyzer optics. The input beam to the polarization optics consisted of a 10-mW He–Ne laser source with an operating wavelength of 0.633 μm. This beam entered an acoustooptic modulator, which provided 100% amplitude modulation of the transmitted radiation with a frequency of about 25 kHz. The modulated laser radiation was then passed through two Glan Thomson linear polarizers. The first polarizer served as an attenuator, while the second polarizer was fixed at 45° with respect to the resulting plane of incidence on the cylindrical surface of the tubular specimen. The laser spot on the specimen was about 1 mm above the target of the multi-wavelength pyrometer. This arrangement eliminated the possibility of stray laser radiation entering the optical system of the pyrometer. The entire source polarization train could be translated for measurements on specimens of different diameters.

The reflected radiation from the specimen was collected by suitable imaging optics and focussed onto a field stop. A portion of this radiation was reflected into a four-quadrant detector, which provided accurate alignment information. When the light was centered in the quadrant, it was also centered in the field stop. Radiation transmitted through the field stop was then recollimated and analyzed by the four-detector polarimeter. The details of the design and construction of the polarimeter have been given elsewhere [4].

The angle of incidence for the ellipsometric measurements was established by placing a custom-built optical prism at the specimen location. The prism was constructed to have two intersecting surfaces whose angle was 70°. The prism was first oriented to reflect the incident laser radiation back onto itself. The laser was then translated to the second surface and the polarimeter was aligned on the reflected beam.

3.5. Data Acquisition System

Voltage signals from the polarimeter and the two pyrometers were digitized using two 16-bit analog-to-digital converter (A-D) cards installed in a personal computer (PC). Each card provided eight channels. The first card was used to digitize the outputs of the four polarization detectors, the outputs of the two channels of the six-wavelength pyrometer, and the output of the one-wavelength pyrometer. The second card was used to digitize the outputs of the quadrant detector.

The data acquisition system was triggered by the computer that controlled the operation of the main current switch. Each set of data, consisting of four polarimeter and three pyrometer signals, was recorded at the rate of 2 kHz.

4. MEASUREMENTS

Measurements were performed on two tubular specimens, one made of molybdenum and one of tungsten. The tubular specimens were fabricated from rod stock. An electroerosion technique was used to bore out the center portion of the rod and to fabricate a small rectangular hole (1×0.5 mm) in the wall at the middle of the specimen. The rectangular hole approximated blackbody conditions for the pyrometer. Nominal dimensions of the specimen were as follows: length, 76 mm; outside diameter, 6.3 mm; and wall thickness, 0.5 mm. The outer surface of the specimen was polished.

The molybdenum specimen was 99.9+% pure. The manufacturer's typical analysis indicated the presence of the following impurities (in ppm, by mass): Fe, 50; Cr and Si, <50 each; C, 40; O, 30; Pb and Ti, <30 each; Al, Ca, Cu, and Mg, <20 each; N and W, 10 each; H, 5; and K, <2.

The tungsten specimen was also 99.9+% pure. The manufacturer's typical analysis indicated the presence of the following impurities (in ppm by mass): Mo, 310; Th, <250; Fe, 60; Zr, 30; Ca and Nb, <20 each; Cu and Ti, 10 each; Al, Cr, and Si, 5 each; and B, Co, Mg, Mn, Ni, Pb, Sn, and Sr, <2 each.

Combined pyrometric and radiometric measurements were performed over the temperature interval 2000 to 2800 K. To optimize the signal resolution of the pyrometers, this interval was divided into two ranges: Range 1, 2000 to 2500 K; and Range 2, 2200 to 2800 K. The higher range was achieved by placing a neutral density filter in the optical path of the pyrometer. In the actual experiments, Range 1 covered 2000 to 2485 K for molybdenum and 2000 to 2400 K for tungsten; Range 2 covered 2200 to 2800 K for both metals. For each metal, two experiments were performed

in each temperature range. The duration of the heating pulse was in the range 480 to 550 ms.

To determine the reproducibility of polarimetric measurements in a given range, eight consecutive experiments were performed on the molybdenum specimen in Range 1.

The pyrometers were calibrated before the start of the measurements in accordance with the procedure described briefly in Section 3.3. Measurements of the transmission of the interference filters in the six-wavelength pyrometer yielded effective wavelengths for the two channels of interest to be 624 and 656 nm. All the experiments were performed with the specimen in a vacuum environment at about 2×10^{-6} Torr ($\approx 3 \times 10^{-4}$ Pa).

5. RESULTS

Data from pyrometric and polarimetric measurements were analyzed to obtain emissivities of molybdenum and tungsten in accordance with the procedures described in Section 2. In the case of the pyrometry technique,

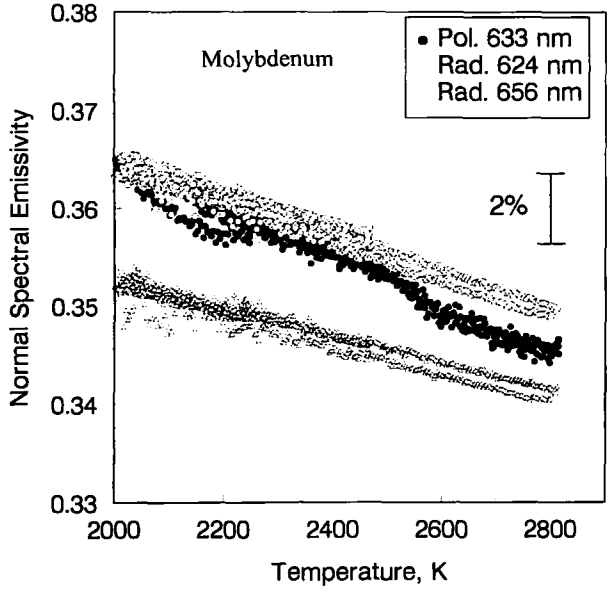

Fig. 3. Normal spectral emissivity of molybdenum determined from radiometric (at 624 and 656 nm) and polarimetric (at 633 nm) measurements.

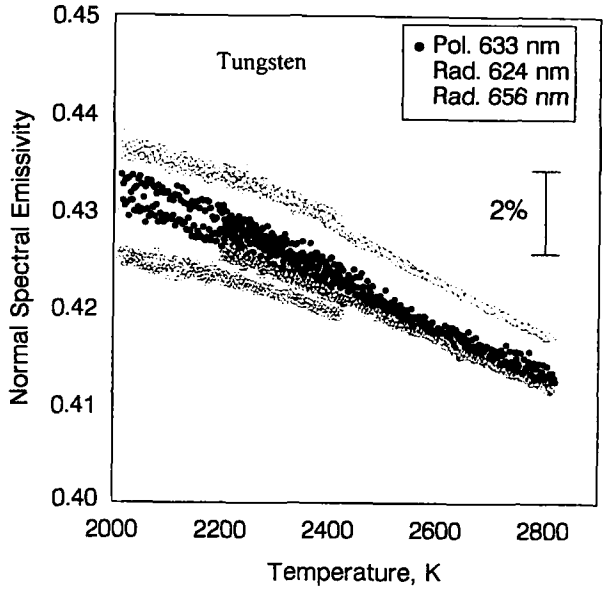

Fig. 4. Normal spectral emissivity of tungsten determined from radiometric (at 624 and 656 nm) and polarimetric (at 633 nm) measurements.

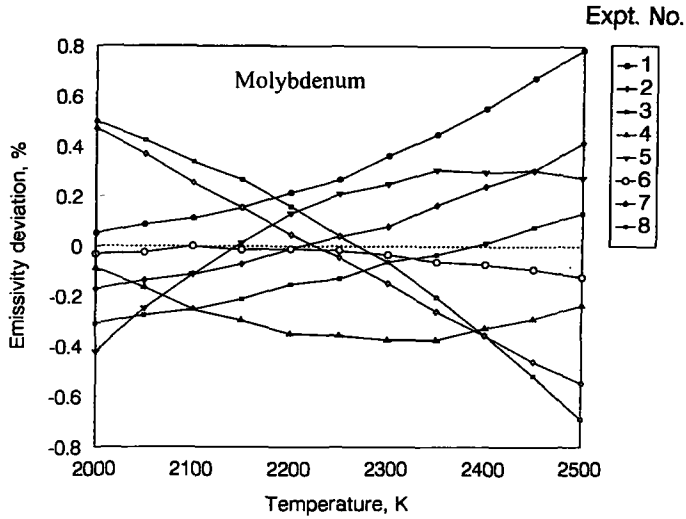

Fig. 5. Deviation of normal spectral emissivity (at 633 nm) results of eight consecutive experiments from their average value for molybdenum determined from polarimetric measurements.

true temperature data were corrected for the quality of the blackbody (calculated to be 99% based on de Vos' method [12]) and for scattered radiation (determined to be 1.6% based on the method described in the literature [7]). Scattered radiation is radiation that enters the optical system of the pyrometer from outside the pyrometer's target area; scattering results mainly from the imperfections of the optical components of the pyrometer. The results on emissivity are given in Figs. 3 and 4 for molybdenum and tungsten, respectively. It may be seen that the results corresponding to 633 nm obtained by the laser polarimetry technique are approximately bracketed by the results corresponding to 624- and 656-mm wavelengths obtained by the pyrometry technique.

The results of eight consecutive experiments on molybdenum, performed to demonstrate reproducibility of the measurements by the polarimetry technique, are shown in Fig. 5. The emissivity data of each experiment were fitted by a quadratic function in temperature by the least squares method. The standard deviation of the data from the function for an experiment was in the range 0.3 to 0.5%. The results, for every 50 K interval, are presented in the form of a deviation plot showing variation of emissivity in an experiment from the average of all the experiments. The results of the eight experiments fell within a bandwidth of considerably less than $\pm 1\%$.

6. ESTIMATES OF UNCERTAINTIES

Estimated uncertainties in the reported emissivities are discussed in terms of uncertainties in the measured quantities as well as of uncertainties due to departure from assumed operational conditions. All uncertainties reported in this paper are based on a two-standard deviation level.

6.1. Uncertainty in Temperature Measurements

Emissivity determined using the pyrometric technique is strongly affected by the uncertainty in temperature measurements since temperature enters directly into the calculation of emissivity [Eq. (3)]. In the case of polarimetry, however, the contribution of uncertainty in temperature to emissivity is small, as it affects only the value of temperature assigned to emissivity.

Uncertainties in radiance temperature measurements with the six-wavelength pyrometer have been discussed in detail in the literature [10]. A summary of the sources of uncertainties and their magnitudes (in parentheses) in the measured radiance temperature relevant to the present work evaluated at about 2400 K (midpoint of the temperature range of the present experiments) follows. It may be noted that when the uncertainties are the same for all the channels, only a single number is given.

(a) Calibration uncertainty of the secondary standard, which in this case is a tungsten-filament lamp (2 K).

(b) Differences in the geometry of the optical system of the pyrometer used to calibrate the standard lamp and the pyrometer used in the present work (0.5 K).

(c) Determination of the effective wavelength of the pyrometer channels (0.5 K at 0.65 μm, 2 K at 0.6 μm).

(d) Nonlinearity in optical and electronic components of the pyrometer (0.5 K).

(e) Calibration transfer from the standard lamp to the pyrometer for the 0.65 μm channel and from the standard lamp to the blackbody furnace and then to the pyrometer for the 0.6-μm channel (1 K at 0.65 μm, 2 K at 0.6 μm).

(f) Alignment of the pyrometer with the radiance source, such as the standard lamp or the specimen (2 K).

(g) Calibration of the neutral density filters (1 K).

(h) Electronic noise and digitization by the analog-to-digital converter (0.5 K).

(i) Drift in pyrometer response (0.5 K).

The resultant total uncertainty in the measured radiance temperature obtained from the square root of the sum of the squares of the various individual uncertainties (rounded upward), for measurements at 0.65 and 0.6 μm, is 4 and 5 K, respectively.

The one-wavelength pyrometer is of a design similar to that of the six-wavelength pyrometer, the major difference being that the former does not have the hexfurcated fiber-optic cable. Therefore, at 0.65 μm, uncertainty in radiance temperature measurements with the one-wavelength pyrometer can be considered to be the same as that of the six-wavelength pyrometer.

The above presentation of uncertainties refers to the measurement of radiance temperature of a surface. In the case of the measurement of the true temperature of the specimen, where the pyrometer is aimed at the blackbody hole in the specimen, additional uncertainties exist. These are due to the uncertainties in the blackbody quality and the scattered radiation mentioned in Section 5. The uncertainty in the calculated blackbody quality is estimated to be 0.5%. The uncertainty in the scattered radiation correction is estimated to be less than 0.5%. At 2400 K, an uncertainty of 0.5% translates into an uncertainty of about 1 K. Since these two uncertainties are relatively small and since the total uncertainties given above were rounded upward, the total reported uncertainties remain unchanged, that is, 4 and 5 K for measurements at 0.65 and 0.6 μm, respectively.

6.2. Uncertainty in Emissivity Determination

Uncertainties in emissivity determinations from radiometric and polarimetric measurements evaluated at about 2400 K are discussed separately in the following sections.

6.2.1. Uncertainty in Emissivity in Radiometric Measurements

Uncertainty in emissivity determination from radiometric measurements can be estimated from uncertainties in the experimental parameters that appear in Eq. (3). These parameters are two temperatures (blackbody and surface radiance) and wavelength. It may be noted that the uncertainties in temperature measurements by the two pyrometers include a significant portion of temperature uncertainties that are of systematic nature common to both pyrometers, such as the uncertainty in the calibration of the standard lamp. Therefore, only a portion of the temperature uncertainties estimated in the previous section makes an appreciable contribution to the uncertainty in emissivity.

To have a realistic determination of these uncertainties, auxiliary experiments were conducted where the tubular specimen was replaced with a molybdenum strip (76 mm in length, 6.3 mm in width, and 0.25 mm in thickness). The two pyrometers were aimed at the same point on the opposite sides of the strip-shaped specimen. Experiments were conducted where the specimen was rapidly heated to high temperatures, similar to those conducted with a tubular specimen. Temperature data from the two pyrometers corresponding to 0.65 μm were, at any given time, in agreement within 1 K. This result corresponds to an uncertainty of about 0.5% in emissivity. Since in the actual experiments one of the pyrometers was aimed at the blackbody hole in the specimen, one should also consider uncertainties in the computed blackbody quality (0.5%) and in the estimated scattered radiation (0.5%). Uncertainty in the calibration of the neutral density filters (1 K), which also needs to be considered, contributed an uncertainty of about 0.5% in emissivity. The major source of uncertainty in emissivity was likely to be due to temperature gradients (axial and radial) in the tubular specimen as well as localized temperature fluctuations due to cross-sectional nonuniformities. These temperature uncertainties may have been as large as 3 K even in the case of precision-machined specimens. This error corresponds to about 1.5% uncertainty in emissivity. Uncertainty in emissivity determinations due to total uncertainties in the measured temperatures was obtained from the square root of the sum of the squares of the individual uncertainties (rounded upward). The resultant uncertainty in emissivity is 1.8% at 0.65 μm. Due to the additional uncertainty

in temperature measurements at 0.6 μm, the corresponding uncertainty in emissivity is estimated to be 1.9%.

Wavelength, λ, is another parameter that appears in Eq. (3). Uncertainty in determining wavelength has been estimated to be not greater than 0.5 nm for the 0.65-μm channel and 2 nm for the 0.6-μm channel [10]. These uncertainties translate into the following uncertainties in emissivity: 0.1% at 0.65 μm and 0.4% at 0.6 μm.

Considering all the uncertainties due to temperature and wavelength determinations, it can be concluded that the total uncertainty in emissivity determination from radiometric measurements was not more than $\pm 2\%$ at both 0.6 and 0.65 μm.

6.2.2. Uncertainty in Emissivity in Polarimetric Measurements

Uncertainty in emissivity determinations from polarimetric measurements resulted mainly from the following three sources: (a) laser radiant flux measurements, (b) instrument calibration, and (c) incidence angle. Since there has not been a long history of the use of this technique, uncertainties in most cases were determined on the basis of realistic estimates of the variation of the parameters that affect operation of the instrument. Estimation of uncertainties due to the above sources was made based on the measurements on molybdenum at 2400 K.

Uncertainty in emissivity arising from uncertainties in radiance measurements by the four detectors and the associated electronic circuits was estimated to be about 0.3%; this was obtained based on variations of about 0.3% in each radiance.

Uncertainty in instrument calibration had two major components: (a) uncertainty in the calibration procedure and (b) drift in calibration over time. To estimate the uncertainty in emissivity due to the uncertainty in the instrument calibration procedure, a 1% numerical variation was applied to selected instrument matrix elements. The instrument matrix was a 4×4 real matrix, which was determined in two steps during the calibration process [4]; the first step determined 12 of the elements and the second determined the remaining 4 elements. To estimate the uncertainty, the 1% variation was applied to either the 12 elements or the 4 elements separately and the resulting uncertainties were averaged over the possible combinations. The results yielded a value of 0.3% for the uncertainty in emissivity due to the uncertainty in the calibration procedure. To estimate the uncertainty in emissivity due to the drift in calibration over time, a drift of about 1% in the sensitivity of the detector–electronics combination was considered. Since the sensitivity of each detector–electronics combination was determined by each row of the instrument matrix, individual rows of the instrument matrix were varied by 1% sequentially and the uncertainties were

computed. The results yielded a value of 1.7% for the uncertainty in emissivity due to the drift in calibration.

The mean angle of incidence of the laser beam was 70°. Uncertainty in this angle was estimated to be about 0.2°, which translates into an uncertainty of about 0.8% in emissivity.

Uncertainty in emissivity due to total uncertainties in the pertinent parameters was obtained from the square root of the sum of the squares of the individual uncertainties. It can be concluded that the total uncertainty in emissivity determination from polarimetric measurements was not more than $\pm 2\%$ at 0.633 μm.

7. DISCUSSION

Linear functions were fitted, by the least-squares method, to the normal spectral emissivity data obtained by both pyrometry and polarimetry

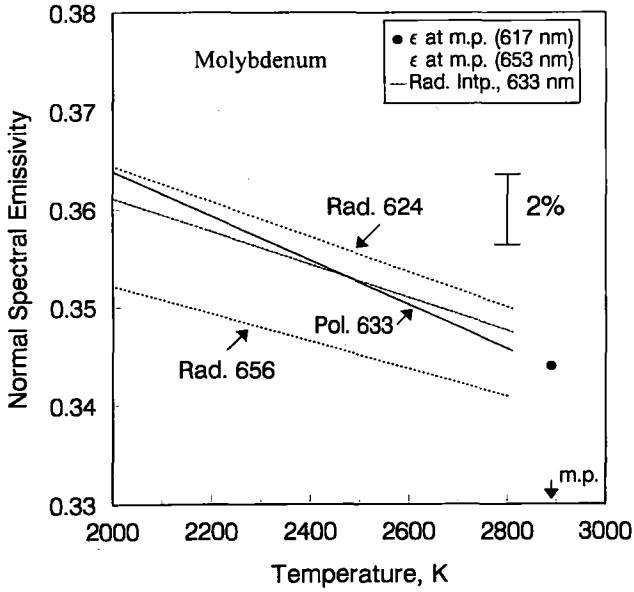

Fig. 6. Smooth curves (linear fits) representing the normal spectral emissivity data on molybdenum given in Fig. 3. Also shown is the curve (identified as Rad. Intp.) that represents emissivity at 633 nm obtained by interpolation between 624- and 656-nm results of the radiometric measurements. Emissivities at the melting point of molybdenum determined earlier in our laboratory [13] are also presented (filled and open circles).

techniques. The resultant curves are shown in Figs. 6 and 7 for molybdenum and tungsten, respectively. Standard deviations are in the range 1.0 to 1.3% for the pyrometric data and 1.3 to 1.6% for the polarimetric data. In both figures, the dotted curve represents normal spectral emissivity values at 633 nm obtained by interpolation between 624- and 656-nm results of the radiometric data. Comparison of this curve with the curve obtained by the laser polarimetry technique at 633 nm indicates that agreement (average absolute difference) is about 0.3% for molybdenum and about 0.7% for tungsten. The maximum deviation between the two curves is about 0.7% for molybdenum and about 0.8% for tungsten.

In Fig. 6, earlier results [13] on normal spectral emissivity at the melting point of molybdenum corresponding to 617 and 653 nm (slightly different wavelengths than those in the present work) are also shown (filled and open circles). It may be noted that extrapolations (less than 100 K) of the present results at the two wavelengths to the melting point yield normal spectral emissivity values about 1.2 and 1.5% higher than the earlier

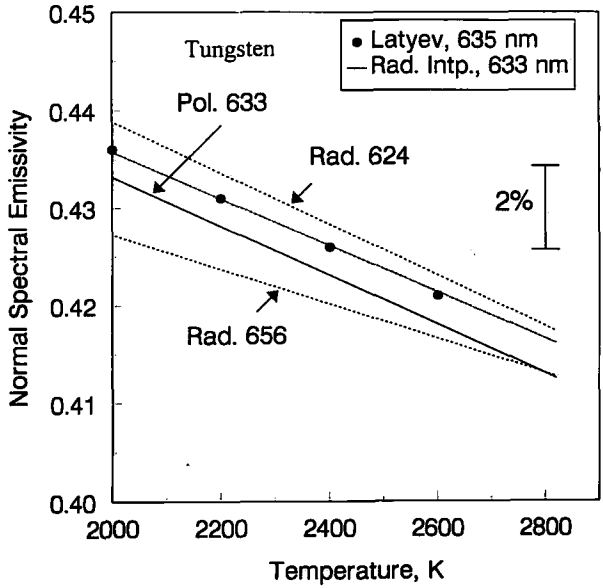

Fig. 7. Smooth curves (linear fits) representing the normal spectral emissivity data on tungsten given in Fig. 4. Also shown is the curve (identified as Rad. Intp.) that represents emissivity at 633 nm obtained by interpolation between 624- and 656-nm results of the radiometric measurements. Emissivity (at 635 nm) results reported by Latyev et al. [14] are also presented (circles).

results. This difference is not unexpected since the surface of polished (solid) molybdenum is not likely to be as smooth as that of molten (liquid) molybdenum, and therefore the solid should have a higher emissivity. A similar comparison was not made for tungsten since an unjustifiably long extrapolation (about 800 K) of the present results would have been required to compare with the results at its melting point. Normal spectral emissivity results for tungsten corresponding to 635 nm reported by Latyev et al. [14] in the overlapping temperature range are shown in Fig. 7 (circles). These results are in very good agreement (within 1%) with those of the present work.

8. CONCLUSIONS

The uncertainty in normal spectral emissivity determined from measurements by either of the two techniques, namely, spectral radiometry or laser polarimetry, is estimated to be not more than $\pm 2\%$. The results of measurements performed on molybdenum and tungsten at high temperatures (2000 to 2800 K) have shown a very good agreement (within 1%) between the normal spectral emissivity values determined by the two independent techniques.

Based on a limited number of experiments, it has been demonstrated that the laser polarimetry technique can be considered to be a valid technique for the accurate measurement of normal spectral emissivity of metals at high temperatures. Measurement of normal spectral emissivity, in addition to surface radiance temperature, permits determination of the true temperature of the specimen. The polarimetry technique has a distinct advantage in cases at high temperatures, where it is either very difficult or impossible to have a blackbody configuration for the specimen to permit direct radiometric (pyrometric) measurement of its true temperature.

ACKNOWLEDGMENTS

This work was supported in part by the Microgravity Science and Applications Division of NASA. The authors also wish to thank P. Nordine of Containerless Research Inc. for his valuable comments and T. Matsumoto, guest scientist from the National Research Laboratory of Metrology (Japan), for his assistance during the conduct of the experiments.

REFERENCES

1. S. Krishnan, G. P. Hansen, R. H. Hauge, and J. L. Margrave, *High. Temp. Sci.* **29**:17 (1990).
2. S. Krishnan and P. C. Nordine, *Phys. Rev. B* **47**:11780 (1993).

3. R. M. A. Azzam and N. M. Bashara, *Ellipsometry and Polarized Light* (North Holland, Amsterdam, 1987).
4. S. Krishnan, *J. Opt. Soc. Am. A* **9**:1615 (1992).
5. R. M. A. Azzam, E. Masetti, I. M. Elminyawi, and F. G. Grosz, *Rev. Sci. Instrum.* **59**:84 (1988).
6. A. Cezairliyan, *J. Res. Natl. Bur. Stand. (U.S.)* **75C**:7 (1971).
7. A. Cezairliyan, M. S. Morse, H. A. Berman, and C. W. Beckett, *J. Res. Natl. Bur. Stand. (U.S.)* **74A**:65 (1970).
8. T. Matsumoto and A. Cezairliyan, in preparation.
9. E. Kaschnitz and A. Cezairliyan, *Int. J. Thermophys.* **17**:1069 (1996).
10. A. Cezairliyan, G. M. Foley, M. S. Morse, and A. P. Miiller, in *Temperature-Its Measurement and Control in Science and Industry, Vol. 6*, J. F. Schooley, ed. (AIP, New York, 1992), pp. 757–762.
11. H. Preston-Thomas, *Metrologia* **27**:3 (1990); **27**:107 (1990).
12. J. C. De Vos, *Physica* **20**:669 (1954).
13. A. P. Miiller and A. Cezairliyan, *Temperature—Its Measurement and Control in Science and Industry, Vol. 6*, J. F. Schooley, ed. (AIP, New York, 1992), pp. 769–774.
14. L. N. Latyev, V. Ya. Chekhovskoi, and E. N. Shestakov, *High Temp. High Press.* **2**:175 (1970).